Feasibility of seismic characterization of multiple fracture sets

Vladimir Grechka* and Ilya Tsvankin†

*Shell International Exploration and Production Inc., Houston, TX; formerly with the Center for Wave Phenomena, Department of Geophysics, Colorado School of Mines.

†Center for Wave Phenomena, Department of Geophysics, Colorado School of Mines.

ABSTRACT

Estimation of parameters of multiple fracture sets is often required for successful exploration and development of naturally fractured reservoirs. The goal of this paper is to determine the maximum number of fracture sets of a certain rheological type which, in principle, can be resolved from seismic data. The main underlying assumption is that an estimate of the complete effective stiffness tensor has been obtained, for example, from multi-azimuth, multi-component surface seismic and VSP data. Although under typical circumstances only a subset of the stiffness elements (or some of their combinations) may be available, this study helps to establish the limits of seismic fracture-detection algorithms.

The number of uniquely resolvable fracture systems depends on the anisotropy of the host rock and the rheology and orientation of the fractures. Somewhat surprisingly, it is possible to characterize fewer vertical fracture sets than dipping ones, even though in the latter case the fracture dip has to be found from the data. For the simplest, rotationally invariant fractures embedded in either a purely isotropic or VTI (transversely isotropic with a vertical symmetry axis) host rock, the stiffness tensor can be inverted for up to *two* vertical or *four* dipping fracture sets. In contrast, only one fracture set of the most general (micro-corrugated) type, regardless of its orientation, is constrained by the effective stiffnesses. These results can serve as a guide for seismic fracture-characterization studies that should take into account the limitations of a particular data set in estimating the effective stiffnesses.

Key words: fracture characterization, stiffness tensor, multicomponent seismic

Introduction

Seismic fracture characterization is critically important in exploration and development of naturally fractured reservoirs which often contain multiple, differently oriented fracture networks (Grimm et al., 1999; Lynn et al., 1999; Pérez et al., 1999). Propagation of elastic waves through fractured media can be effectively described by the linear-slip theory suggested by Schoenberg (1980, 1983) and further refined by Schoenberg and Muir (1989) and Schoenberg and Sayers (1995). This theory is designed to compute the compliance matrix of the effective anisotropic medium containing one or more systems of aligned fractures by adding the compliances of each fracture set to that of the background. Despite several simplifying assumptions (such as neglecting the interaction between fracture sets), the linear-slip formalism can be effectively used to model and invert effective elastic parameters in seismic fracture detection and characterization.

Since fractured reservoirs are azimuthally anisotropic, their comprehensive characterization requires acquisition of wide-azimuth, multicomponent seismic data. Processing of reflected waves produces such signatures as the NMO (normal-moveout) ellipses of different modes, amplitude variation with offset and azimuth, and shear-

wave polarizations and splitting coefficients. Additionally, walkaway VSP (vertical seismic profiling) data can be used to estimate slowness surfaces and polarization vectors at receiver locations in boreholes. Available combinations of those signatures can be inverted for the effective stiffness (or compliance) coefficients of fractured rock. Then the linear-slip theory can be employed to infer the fracture compliances and orientations for a certain fracture model from the obtained stiffness (compliance) matrix. This approach is discussed in detail by Bakulin, Grechka and Tsvankin (2000a,b,c, 2002), who developed a number of practical seismic fracture-characterization algorithms for typical anisotropic models with one or two vertical fracture sets.

Estimation of fracture parameters from seismic data, however, cannot always be accomplished in a unique fashion. As noted by Bakulin, Grechka and Tsvankin (2000a), effective anisotropic media are fully described by up to 21 stiffness coefficients (the number for the most general, triclinic symmetry), whereas the number of fracture parameters for multiple fracture sets and low symmetries of the background rock can become arbitrarily large. Therefore, there exists a *finite* subset of fractured models (containing a relatively small number of fracture systems) which can be unambiguously characterized based on seismic data. In fact, the class of such fractured media is limited not just by the number of unknown fracture parameters. An elaborate analysis of the stiffness tensor shows that several compliances of differently oriented fracture sets may contribute to the same effective stiffness coefficient (e.g., Bakulin et al., 2002). As a result, it is possible to resolve only particular combinations of those compliances, rather than their individual values.

The goal of this paper is to identify fracture sets whose compliances and orientations can be unambiguously determined from the effective stiffness tensor. We examine three different rheological types of fractures – rotationally invariant, diagonal* and completely general (Grechka et al., 2001). The fractures are embedded in either a purely isotropic or VTI (transversely isotropic with a vertical symmetry axis) host rock, with each fracture set arbitrarily oriented in 3-D space. Throughout the paper, we assume an ideal scenario when all 21 stiffness coefficients have been estimated, for example, from multiazimuth walkaway P- and S-wave VSP data or from a combination of surface and VSP data (e.g., Bakulin, Slater, Bunain, and Grechka, 2000; Horne and Leaney, 2000; Grechka et al., 2001; Dewangan and Grechka, 2002). By computing the Frechèt derivatives of the effective stiffness coefficients with respect to the fracture and background parameters, we determine how many different fracture sets of a certain type (along with the unknown background parameters) are constrained by the stiffness matrix. This analysis reveals the dependence of the maximum number of resolvable fracture systems on the rheology and orientation of the fractures, as well as on the presence of anisotropy in the background.

* Such fractures are called orthotropic by Schoenberg and Helbig (1997).

Effective stiffness of fractured rock

General relationships

According to the linear-slip theory (Schoenberg, 1980, 1983; Nichols et al., 1989; Schoenberg and Sayers, 1995), the effective compliance matrix $\boldsymbol{s}$ of a medium containing N sets of aligned fractures is given by

$$\boldsymbol{s} = \boldsymbol{s}_b + \sum_{i=1}^{N} \boldsymbol{s}_f^{(i)}, \qquad (1)$$

where $\boldsymbol{s}_b$ and $\boldsymbol{s}_f^{(i)}$ are the 6×6 symmetric compliance matrices of the unfractured background and the ith fracture set, respectively. By definition, the effective stiffness matrix $\boldsymbol{c}$ is the inverse of the compliance matrix:

$$\boldsymbol{c} = \boldsymbol{s}^{-1} = \left(\boldsymbol{s}_b + \sum_{i=1}^{N} \boldsymbol{s}_f^{(i)} \right)^{-1} = \left(\boldsymbol{c}_b^{-1} + \sum_{i=1}^{N} \boldsymbol{s}_f^{(i)} \right)^{-1}; \qquad (2)$$

$\boldsymbol{c}_b$ is the stiffness matrix of the host rock.

Here, we examine two types of the background medium: isotropic (denoted as ISO) and transversely isotropic with a vertical axis of symmetry (VTI). Using the Lamé parameters λ and μ, the isotropic stiffness matrix can be written as

$$\boldsymbol{c}_b^{\mathrm{ISO}} = \begin{pmatrix} \lambda+2\mu & \lambda & \lambda & 0 & 0 & 0 \\ \lambda & \lambda+2\mu & \lambda & 0 & 0 & 0 \\ \lambda & \lambda & \lambda+2\mu & 0 & 0 & 0 \\ 0 & 0 & 0 & \mu & 0 & 0 \\ 0 & 0 & 0 & 0 & \mu & 0 \\ 0 & 0 & 0 & 0 & 0 & \mu \end{pmatrix}. \qquad (3)$$

For VTI media,

$$\mathbf{c}_b^{\mathrm{VTI}} = \begin{pmatrix} c_{11b} & c_{12b} & c_{13b} & 0 & 0 & 0 \\ c_{12b} & c_{11b} & c_{13b} & 0 & 0 & 0 \\ c_{13b} & c_{13b} & c_{33b} & 0 & 0 & 0 \\ 0 & 0 & 0 & c_{44b} & 0 & 0 \\ 0 & 0 & 0 & 0 & c_{44b} & 0 \\ 0 & 0 & 0 & 0 & 0 & c_{66b} \end{pmatrix}, \qquad (4)$$

where $c_{12b} = c_{11b} - 2\,c_{66b}$.

The matrices $\mathbf{c}_b^{\mathrm{ISO}}$ and $\mathbf{c}_b^{\mathrm{VTI}}$ are written in a certain "global" Cartesian coordinate frame $\{x_1, x_2, x_3\}$ used below to describe both the background and embedded fractures. Whereas the orientation of this frame can be

arbitrary when the host rock is isotropic, in the case of the VTI background the x_3-axis is taken parallel to the symmetry axis of the medium.

Excess fracture compliance

The excess compliance of the most general (micro-corrugated) fracture set with the normal in the x_1-direction is described by the following 6×6 symmetric matrix (Schoenberg, 1980; Bakulin et al., 2000c; Grechka et al., 2001):

$$\boldsymbol{s}_f^{\mathrm{GN},\,x_1} = \begin{pmatrix} K_N & 0 & 0 & 0 & K_{NV} & K_{NH} \\ 0 & 0 & 0 & 0 & 0 & 0 \\ 0 & 0 & 0 & 0 & 0 & 0 \\ 0 & 0 & 0 & 0 & 0 & 0 \\ K_{NV} & 0 & 0 & 0 & K_V & K_{VH} \\ K_{NH} & 0 & 0 & 0 & K_{VH} & K_H \end{pmatrix}, \qquad (5)$$

The nonzero off-diagonal elements of the matrix $\boldsymbol{s}_f^{\mathrm{GN},\,x_1}$ imply the existence of coupling between the slips (jumps in displacement across the fractures) and tractions in the directions normal and tangential to the fractures. It can be shown (Berg et al., 1991) that any rotation of the fracture plane around the x_1-axis does not change the form of the matrix $\boldsymbol{s}_f^{\mathrm{GN},\,x_1}$. However, if the fracture normal deviates from the x_1-axis, the excess fracture compliance matrix $\boldsymbol{s}_f^{\mathrm{GN},\,n}$ in the fixed coordinate frame may no longer contain any vanishing elements. We describe the fracture normal $\boldsymbol{n}$ by its azimuth α and dip (or tilt) β (Figure 1):

$$\boldsymbol{n} = \{\cos\alpha\,\cos\beta,\ \ \sin\alpha\,\cos\beta,\ \ -\sin\beta\,\}\,, \qquad (6)$$

Exact expressions for the elements of the matrix $\boldsymbol{s}_f \equiv \boldsymbol{s}_f^{\mathrm{GN},\,n}$ in terms of the angles α and β are given in Appendix A [equations (A4)–(A24)]. Those equations are essential for the problem at hand because they represent the most general excess fracture compliance matrix allowed by the linear-slip theory. The compliance matrices for fracture sets with any particular rheology or orientation can be obtained as special cases of the matrix $\boldsymbol{s}_f$. For instance, equations (2) of Schoenberg et al. (1999) for vertical fractures with a diagonal compliance matrix follow from equations (A4)–(A24) by simply setting $K_{NV} = K_{NH} = K_{VH} = 0$ and $\beta = 0$.

For fractures with a less complicated rheology, slips in the direction normal to the fracture plane ("normal slips") are decoupled from tractions in the perpendicular direction, tangential to the fractures ("tangential tractions"). Similarly, tangential slips for those fractures are decoupled from normal tractions. Then, in a certain coordinate frame the excess fracture compliance matrix (5) becomes diagonal. Therefore, we call fractures of this type "diagonal" and denote them with the superscript DI. It should be noted, however, that the compliance

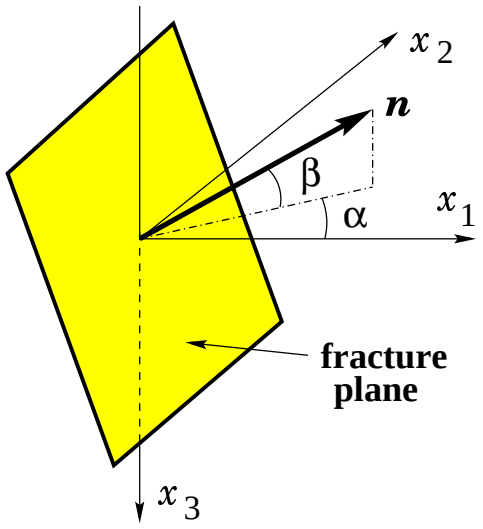

Figure 1. Orientation of a fracture set is defined by the azimuth α and dip β of the unit vector $\boldsymbol{n}$ orthogonal to the fracture plane.

matrix $\boldsymbol{s}_f^{\mathrm{DI},\,x_1}$ of diagonal fractures acquires a nonzero off-diagonal element $s_{56f}^{\mathrm{DI},\,x_1}$ after an arbitrary rotation around the fracture normal (i.e., the x_1-axis). Thus, the compliance matrix of diagonal fractures is given by

$$\boldsymbol{s}_f^{\mathrm{DI},\,x_1} = \begin{pmatrix} K_N & 0 & 0 & 0 & 0 & 0 \\ 0 & 0 & 0 & 0 & 0 & 0 \\ 0 & 0 & 0 & 0 & 0 & 0 \\ 0 & 0 & 0 & 0 & 0 & 0 \\ 0 & 0 & 0 & 0 & K_V & K_{VH} \\ 0 & 0 & 0 & 0 & K_{VH} & K_H \end{pmatrix}. \qquad (7)$$

To make the matrix $\boldsymbol{s}_f^{\mathrm{DI},\,x_1}$ diagonal, the coordinate frame has to be rotated by the angle $\nu = (1/2)\,\tan^{-1}\left[2\,K_{VH}/(K_V - K_H)\right]$ around the x_1-axis. Equations (A4)–(A24) of Appendix A yield the compliance matrix of diagonal fractures orthogonal to the vector $\boldsymbol{n}$ [equation (6)] if one substitutes

$$K_{NV} = K_{NH} = 0\,. \qquad (8)$$

The simplest type of fractures, called "rotationally invariant" (RI in our notation) by Schoenberg and Sayers (1995), corresponds to diagonal fractures with equal tangential compliances $K_V = K_H$:

$$\boldsymbol{s}_f^{\mathrm{RI},\,x_1} = \begin{pmatrix} K_N & 0 & 0 & 0 & 0 & 0 \\ 0 & 0 & 0 & 0 & 0 & 0 \\ 0 & 0 & 0 & 0 & 0 & 0 \\ 0 & 0 & 0 & 0 & 0 & 0 \\ 0 & 0 & 0 & 0 & K_V & 0 \\ 0 & 0 & 0 & 0 & 0 & K_V \end{pmatrix}. \qquad (9)$$

Any rotation around the fracture normal (i.e., around the x_1-axis) does not change the form of the matrix (9).

Host rock		Fracture set		
ISO	VTI	RI	DI	GN
2	5	4	6	8

Table 1. Number of independent parameters needed to describe isotropic (ISO) and VTI background media, as well as rotationally invariant (RI), diagonal (DI) and general (GN) fractures. The numbers for the fracture sets include the orientation angles α and β.

Hence, the compliance $\boldsymbol{s}_f^{\mathrm{RI},\,n}$, of a rotationally invariant fracture set with the normal $\boldsymbol{n}$ can be found from equations (A4)–(A24) after the following substitutions:

$$K_{NV} = K_{NH} = K_{VH} = 0 \quad \text{and} \quad K_H = K_V\,. \tag{10}$$

Table 1 lists the number of independent physical model parameters for the two types of host rock (background) and three types of fracture systems considered above. For a given number and type of fracture sets embedded in a certain background, the dimension of the composite parameter space is equal to the sum of the dimensions of the individual parameter spaces. For example, the effective medium formed by two rotationally invariant fracture sets embedded in a purely isotropic background is described by a total of $2 \times 4 + 2 = 10$ independent parameters.

Since fracture characterization can be unique only if there are no more than 21 physical parameters (the number of stiffness coefficients for the most general, triclinic symmetry), Table 1 helps to identify fractured models that cannot (even in principle) be constrained by seismic data. For instance, it is impossible to estimate the parameters of three arbitrarily oriented diagonal fracture sets in a VTI host rock because the total number of parameters in this case is $3 \times 6 + 5 = 23 > 21$.

Frechèt derivatives of the effective stiffness matrix

Although Table 1 provides useful insight into the fracture-characterization problem, it only shows that for a certain class of models the number of constraints is smaller than the number of unknowns, so the fracture and background parameters cannot be resolved. However, even if the number of effective stiffness coefficients is larger than the number of unknown physical parameters, the inversion for a particular parameter can still be ambiguous.

To study the uniqueness of the inverse problem, we apply the singular value decomposition (SVD) to the matrix of Frechèt derivatives of the effective stiffnesses $\boldsymbol{c}$ with respect to the unknown model parameters. The model parameter vector $\boldsymbol{m}$ can be represented as

$$\boldsymbol{m} \equiv \boldsymbol{b} \bigcup \boldsymbol{f}^{(1)} \bigcup \ldots \bigcup \boldsymbol{f}^{(N)}\,, \tag{11}$$

where $\boldsymbol{b}$ includes the background stiffnesses and $\boldsymbol{f}^{(1)}, \ldots, \boldsymbol{f}^{(N)}$ are vectors of the independent excess fracture compliances [equations (5), (7) or (9)] and the orientation angles of each fracture set. The necessary prerequisite for a unique inversion discussed above is

$$\dim \boldsymbol{m} = \dim \boldsymbol{b} + \sum_{i=1}^{N} \dim \boldsymbol{f}^{(i)} \le 21\,, \tag{12}$$

where "$\dim \boldsymbol{v}$" denotes the dimension of each vector.

The matrix of Frechèt derivatives can be obtained by differentiating equation (2):

$$\begin{aligned}
\mathcal{F} \equiv \frac{\partial \boldsymbol{c}}{\partial \boldsymbol{m}} &= \frac{\partial}{\partial \boldsymbol{m}} \left[\left(\boldsymbol{c}_b^{-1} + \sum_{i=1}^{N} \boldsymbol{s}_f^{(i)} \right)^{-1} \right] \\
&= -\left(\boldsymbol{c}_b^{-1} + \sum_{i=1}^{N} \boldsymbol{s}_f^{(i)} \right)^{-1} \left(-\boldsymbol{c}_b^{-1} \frac{\partial \boldsymbol{c}_b}{\partial \boldsymbol{m}} \boldsymbol{c}_b^{-1} \right. \\
&\qquad \left. + \sum_{i=1}^{N} \frac{\partial \boldsymbol{s}_f^{(i)}}{\partial \boldsymbol{m}} \right) \left(\boldsymbol{c}_b^{-1} + \sum_{i=1}^{N} \boldsymbol{s}_f^{(i)} \right)^{-1}\,.
\end{aligned} \tag{13}$$

Applying equation (2) again yields

$$\begin{aligned}
\mathcal{F} &= \boldsymbol{c} \left(\boldsymbol{c}_b^{-1} \frac{\partial \boldsymbol{c}_b}{\partial \boldsymbol{m}} \boldsymbol{c}_b^{-1} - \sum_{i=1}^{N} \frac{\partial \boldsymbol{s}_f^{(i)}}{\partial \boldsymbol{m}} \right) \boldsymbol{c} \\
&= \boldsymbol{c} \left(\boldsymbol{s}_b \frac{\partial \boldsymbol{c}_b}{\partial \boldsymbol{m}} \boldsymbol{s}_b - \sum_{i=1}^{N} \frac{\partial \boldsymbol{s}_f^{(i)}}{\partial \boldsymbol{m}} \right) \boldsymbol{c}\,.
\end{aligned} \tag{14}$$

Note that all derivatives in equation (14) are easy to find in explicit form because the stiffness matrix $\boldsymbol{c}_b$ is differentiated only with respect to the stiffness coefficients of the host rock [i.e., to the portion $\boldsymbol{b}$ of the vector $\boldsymbol{m}$, see equation (11)], while the compliance matrices $\boldsymbol{s}_f^{(i)}$ are differentiated only with respect to the fracture compliances and orientations (i.e., to the portions $\boldsymbol{f}^{(i)}$ of $\boldsymbol{m}$). Indeed, $\boldsymbol{c}_b$ is independent of $\boldsymbol{s}_f^{(i)}$, so the corresponding derivative $\partial \boldsymbol{c}_b / \partial \boldsymbol{f}^{(i)} = 0$ for any i; likewise, $\partial \boldsymbol{s}_f^{(i)} / \partial \boldsymbol{b} = 0$ and, if $i \neq j$, $\partial \boldsymbol{s}_f^{(i)} / \partial \boldsymbol{f}^{(j)} = 0$. Clearly, the Frechèt matrix $\mathcal{F}$, which has the dimension $21 \times \dim \boldsymbol{m}$, is sparse because so many derivatives in equation (14) go to zero.

Analysis of the Frechèt matrix

To answer the question whether it is possible to estimate the parameter vector $\boldsymbol{m}$ from the measured stiffness coefficients $\boldsymbol{c}$, we perform singular value decomposition of the matrix $\mathcal{F}$. According to the standard SVD criterion, if the condition number (defined as the ratio

	RI	DI	GN
ISO	4	3	1
VTI	4°	2	1

Table 2. Maximum number of dipping fracture sets that can be uniquely resolved from the stiffness matrix.

of the greatest singular value to the smallest one) of $\mathcal{F}$ is finite,

$$\kappa \equiv \operatorname{cond} \mathcal{F} < \infty , \tag{15}$$

the inversion for $\boldsymbol{m}$ is theoretically unique (for noise-free data). Estimation of $\boldsymbol{m}$ becomes ambiguous (non-unique) if

$$\kappa = \infty . \tag{16}$$

To identify the maximum possible number of fracture sets which can be resolved using the effective stiffness coefficients, we elected the following simple approach. After choosing the symmetry of the host rock (isotropic or VTI), we keep adding fracture sets of a certain type to the model until the condition number becomes "infinite." In the tests below, κ is considered infinite if it exceeds the numerical limit set in the Matlab software ($2^{2^{10}} \approx 1.8 \cdot 10^{308}$).

Arbitrarily oriented (dipping) fractures

The analysis of the condition number for fracture sets with arbitrary dip and azimuth is summarized in Table 2. The results show an intuitively obvious trend: the more complicated rheology the fracture systems have, the fewer such systems can be uniquely estimated from the effective stiffnesses. It is interesting that for rotationally invariant and diagonal fractures it should be possible to invert for as many fracture sets as allowed by the dimensionality constraint (12). In contrast, the stiffness matrix can be inverted for the parameters of only *one* general fracture set, even for the simplest isotropic background rock.

Obviously, a finite value of the condition number indicates the possibility of inverting a *complete*, 21-element stiffness matrix for the medium parameters. Estimating the stiffness matrix itself is a highly challenging problem that typically requires acquisition and processing of multi-component, multi-azimuth data. Despite a significant progress recently achieved in the inversion for transversely isotropic (e.g., Horne and Leaney, 2000; Tsvankin and Grechka, 2000a,b; Bakulin, Grechka and Tsvankin, 2000a; Tsvankin, 2001), orthorhombic (Grechka et al., 1999; Bakulin, Grechka and Tsvankin, 2000b) monoclinic (Grechka et al., 2000; Bakulin, Grechka and Tsvankin, 2000c) and even triclinic (Grechka et al., 2001; Dewangan and Grechka, 2002) media, parameter estimation for lower anisotropic symmetries requires further development.

In particular, seismic signatures needed for characterization of dipping fractures have seldom been discussed in the literature. A relatively simple model with a single set of dipping rotationally invariant fractures in a VTI host rock (this model is marked with the diamond in Table 2) was analyzed by Grechka and Tsvankin (2001). The effective model in this case has monoclinic symmetry with a vertical symmetry plane parallel to the dip plane of the fractures. Grechka and Tsvankin (2001) showed that all fracture and background parameters can be obtained from the vertical velocities and NMO ellipses of PP-waves and two split SS-waves (or mode-converted waves) reflected from horizontal interfaces.

The analysis of the Frechèt matrix indicates that it is possible to resolve a total of *four* systems of rotationally invariant fractures in a VTI background. Such a model has the maximum possible number of independent physical parameters (21), all of which can be estimated from the stiffness matrix of the effective triclinic medium.

Figure 2 shows a typical example of the relationship between the condition number κ and the fracture dip β for a model that includes three rotationally invariant fracture sets. For a wide range of dips the curve is almost flat with the condition number satisfying $10^2 < \kappa < 10^3$, which indicates that the inverse problem is well-posed (according to our criterion). Only for dips extremely close to 0° and 90 ° (i.e., for near-vertical and near-horizontal fractures) does the condition number rapidly go to infinity. The parameter-estimation problem for vertical fractures is discussed in detail in the next section. Horizontal fractures are not typical for naturally fractured reservoirs and will not be analyzed further.

Vertical fractures

Most existing papers on fracture characterization treat vertical fracture networks which are believed to be common for naturally fractured reservoirs. To establish the maximum number of vertical fracture networks that can be characterized by seismic data, we set the fracture tilt β (Figure 1) to zero and assume that it is known *a priori*. Although it seems that making the fractures vertical should help in fracture detection because each set is described by one fewer parameter, Table 3 proves this expectation to be wrong. For the simplest, rotationally invariant fractures in both isotropic and VTI background, the maximum number of resolvable vertical fracture sets is just two compared to four dipping sets in Table 2.

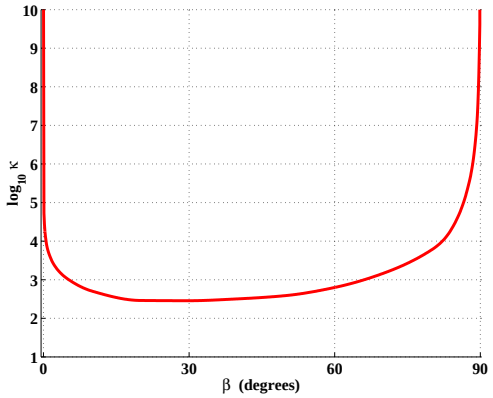

Figure 2. The influence of fracture dip on the condition number κ of the Frechèt matrix for the model of three rotationally invariant fracture sets in a purely isotropic background with $V_P/V_S = 2$. The dip β (the x-axis of the plot) is the same for all three sets. For the first set, $K_N^{(1)} = 0.11$ (all compliances are density-normalized and given in $\mathrm{s}^2/\mathrm{km}^2$), $K_V^{(1)} = 0.18$, and the azimuth of the fracture normal $\alpha^{(1)} = 0°$; for the second set, $K_N^{(2)} = 0.15$, $K_V^{(2)} = 0.13$, and $\alpha^{(2)} = 60°$; for the third set, $K_N^{(3)} = 0.16$, $K_V^{(3)} = 0.19$, and $\alpha^{(3)} = 120°$.

	RI	DI	GN
ISO	$2^{\star}$	2	$1^{\ddagger}$
VTI	$2^{\star\star}$	$2^{\dagger}$	1

Table 3. Maximum number of vertical fracture sets that can be uniquely resolved from the stiffness matrix.

To explain this paradox, note that fixing the tilt of fractures ($\beta = 0$) removes one degree of freedom in the description of each fracture set. As a consequence, certain excess compliances of different fracture systems can map into the same element of the effective stiffness matrix, which making estimation of these individual compliances impossible. An example of this type of ambiguity is discussed by Bakulin et al. (2001) for orthogonal vertical fracture sets in a VTI host rock (see below).

The simplest fractured model is that of vertical rotationally invariant fractures in an otherwise isotropic host rock (marked with a star in Table 3). For a single fracture set, the effective medium is transversely isotropic with a horizontal symmetry axis (e.g., Schoenberg and Sayers, 1995; Bakulin, Grechka and Tsvankin, 2000a). Fracture-characterization algorithms for this model, presented by Bakulin, Grechka and Tsvankin (2000a), can be based entirely on surface reflection data. Two vertical fracture systems making an arbitrary angle with each other lower the effective medium symmetry to monoclinic (the only symmetry plane of the model is horizontal). In the special case of orthogonal fracture sets, the effective model is orthorhombic, with the vertical symmetry planes parallel to the fracture strike directions. For both models with two vertical fracture sets, the fracture and background parameters can be estimated from the vertical velocities and NMO ellipses of PP- and two split SS-waves (or converted PS-waves) from horizontal interfaces (Bakulin, Grechka and Tsvankin, 2000b,c).

Two vertical fracture sets in a VTI background (two stars in Table 3) also yield an effective monoclinic medium with a horizontal symmetry plane. Bakulin et al. (2002) showed that if the fractures are rotationally invariant and the sets are orthogonal (then the effective medium is orthorhombic), the fracture and background parameters cannot be estimated in a unique fashion. Although the number of the physical parameters in this model is equal to the number of non-zero effective stiffnesses (nine), there is an additional relation (constraint) between the stiffnesses or Tsvankin's (1997) anisotropic coefficients that causes the ambiguity.

While this conclusion is correct, our study reveals that the orthogonal orientation of the fracture systems is the *only* special case for this model when the Frechèt matrix $\mathcal{F}$ degenerates. As illustrated by Figure 3, the condition number κ rapidly increases only when the angle $\Delta\alpha$ between the fractures is in a narrow vicinity of 0° (parallel sets) or 90° (orthogonal sets). Even if $\Delta\alpha$ deviates by just a few degrees from 90°, the inversion should be feasible, and the stiffnesses of the effective monoclinic medium (this model is similar to the one described by Bakulin et al., 2000c) can be used to constrain the fracture and the background parameters.

A single system of vertical diagonal fractures [equation (7)] with $K_{VH} = 0$ in a VTI host rock (the dagger in Table 3) creates an effective orthorhombic medium (Schoenberg and Helbig, 1997). Bakulin et al. (2000b) showed that the fracture compliances and orientations for this model can be estimated from PP and SS (or PS) reflection data. The inversion for the VTI background parameters also requires knowledge of the vertical velocities or reflector depth. Moreover, Table 3 indicates that the parameter estimation is still possible for two sets of diagonal fractures in both isotropic and VTI background. Estimation of the compliances of two fracture sets, however, cannot be performed without using multiazimuth VSP data.

Characterization of vertical fractures of the most general type embedded in a purely isotropic host rock (the double dagger in Table 3) was studied by Grechka et al. (2001). Despite the lowest possible (triclinic) symmetry of the effective model, Grechka et al. (2001) prove

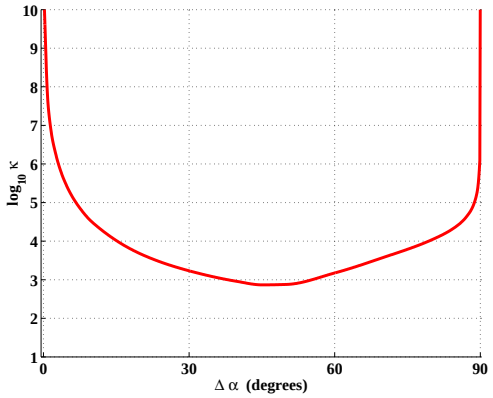

Figure 3. The condition number κ for the model of two vertical, rotationally invariant fracture sets in a VTI background. $\Delta\alpha$ denotes the difference between the fracture azimuths. The compliances are $K_N^{(1)} = 0.15$, $K_V^{(1)} = 0.14$, $K_N^{(2)} = 0.13$, and $K_V^{(2)} = 0.12$. The density-normalized background stiffnesses are (in $\mathrm{km}^2/\mathrm{s}^2$) are $c_{11} = 3.90$, $c_{33} = 4.00$, $c_{44} = 1.00$, $c_{66} = 1.19$, $c_{13} = 1.71$.

that the fracture and background parameters can be inverted from a combination of reflection and borehole data that includes the vertical velocities and NMO ellipses of PP- and SS-waves supplemented with P-wave multi-azimuth walkaway VSP data. Addition of another general fracture system makes the inversion ambiguous, although the number of independent physical parameters for either background still does not exceed 21.

Discussion and conclusions

Seismic estimation of the parameters of multiple fracture sets embedded in an otherwise isotropic or VTI background is an important practical issue in characterization and development of naturally fractured reservoirs. Although our approach can be applied to other types of the host rock (i.e., orthorhombic or monoclinic), such low background symmetries can be caused only by the intrinsic anisotropy of the rock-forming crystals. Since crystal anisotropy is known to be untypical for relatively shallow layers important in seismic exploration, we decided to exclude those more complicated background models from consideration.

The key assumption in our study was that all elements of the effective stiffness matrix $\boldsymbol{c}$ can be recovered from seismic data. By expressing the stiffnesses through the fracture and background parameters and analyzing the condition number of the corresponding Frechèt matrix, we determined the maximum number of fracture sets with a given rheology which can be uniquely resolved under those "ideal" conditions. If the fracture sets are tilted away from the vertical (i.e., the fractures are dipping), it may be possible to characterize up to four rotationally invariant fracture sets in either isotropic or VTI background. Surprisingly, parameter estimation becomes more ambiguous for vertical fractures which create simpler (i.e., higher-symmetry) effective anisotropic models. Because of the trade-offs between different fracture parameters which contribute to $\boldsymbol{c}$ only in certain combinations, no more than two vertical fracture sets can be resolved from the effective stiffnesses. Even a small fracture dip, however, is sufficient to sharply reduce the condition number and make the inverse problem much better posed.

In practice, estimation of fracture parameters has to be based on available (incomplete) data which usually cannot constrain all stiffness coefficients c_{ij} individually. This is particularly true for lower anisotropic symmetries (such as triclinic) described by up to 21 independent stiffnesses. Inversion of field data may yield only combinations of some stiffness elements, while information about other stiffnesses may be missing entirely. Such incomplete stiffness matrix may constrain fewer fracture sets than indicated by our analysis (if any), so it may become necessary to impose restrictions on the fracture rheology (e.g., assume rotationally invariant fractures) and orientation, or ignore the background anisotropy. In principle, a feasibility study similar to the one described here can be carried out for any given set of available seismic data or effective stiffness coefficients.

Another reason for our results to be overly optimistic is that we deem the inversion to be non-unique only when the condition number of the Frechèt matrix goes to infinity. Therefore, the entries in Tables 2 and 3 formulated in a "yes/no" fashion should be regarded with caution. In fact, there is a vast "transitional" set of models with relatively large condition numbers that requires a special treatment. For instance, according to the view taken in our paper, two fracture sets making a small angle with each other may still be resolvable if the corresponding condition number is finite (see Figure 3). However, this is not necessarily true in practice, when the effective stiffness coefficients are estimated with a certain error. It is clear from both the physics and mathematics of the linear-slip theory that if the angle between two fracture sets is smaller than a certain value (that depends on errors in c_{ij}), they appear as a single set with the total excess compliance equal to the sum of the corresponding individual compliances. This issue can be accounted for in our study by using a more conservative condition ($\mathrm{cond}\,\mathcal{F} > M$, where M is a positive number) to define nonuniqueness.

Acknowledgments

We are grateful to Roel Snieder and Reynaldo Cardona (both CSM) for their reviews of the manuscript.

References

Bakulin, A., Grechka, V., and Tsvankin, I., 2000a, Estimation of fracture parameters from reflection seismic data – Part I: HTI model due to a single fracture set: Geophysics, **65**, 1788–1802.

Bakulin, A., Grechka, V., and Tsvankin, I., 2000b, Estimation of fracture parameters from reflection seismic data – Part II: Fractured models with orthorhombic symmetry: Geophysics, **65**, 1803–1817.

Bakulin, A., Grechka, V., and Tsvankin, I., 2000c, Estimation of fracture parameters from reflection seismic data – Part III: Fractured models with monoclinic symmetry: Geophysics, **65**, 1818–1830.

Bakulin, A., Slater, C., Bunain, H., and Grechka, V., 2000, Estimation of azimuthal anisotropy and fracture parameters from multiazimuthal walkaway VSP in the presence of lateral heterogeneity: 70th Ann. Internat. Mtg., Soc. Expl. Geophys., Expanded Abstracts, 1405–1408.

Bakulin, A., Grechka, V., and Tsvankin, I., 2002, Seismic inversion for the parameters of two orthogonal fracture sets in a VTI background medium: Geophysics, **67**, 289–296.

Berg, E., Hood, J., and Fryer, G., 1991, Reduction of the general fracture compliance matrix Z to only five independent elements: Geophys. J. Int., **107**, 703–707.

Dewangan, P., and Grechka, V., 2002, Inversion of multicomponent, multi-azimuth, walkaway VSP data for the stiffness tensor: CWP Research Report, this volume.

Grechka, V., Bakulin, A., and Tsvankin, I., 2001, Seismic signatures of vertical fractures described as general linear-slip interfaces: CWP Research Report CWP–368 (also Geophys. Prosp., submitted).

Grechka, V., Contreras, P., and Tsvankin, I., 2000, Inversion of normal moveout for monoclinic media: Geophysical Prospecting, **48**, 577–602.

Grechka, V., Theophanis, S., and Tsvankin, I., 1999, Joint inversion of P- and PS-waves in orthorhombic media: Theory and a physical-modeling study: Geophysics, **64**, 146–161.

Grechka, V., and Tsvankin, I., 2001, Characterization of dipping fractures in transversely isotropic background: CWP Research Report CWP–369 (also Geophys. Prosp., submitted).

Grimm, R.E., Lynn, H.B., Bates, C.R., Phillips, D.R., Simon, K.M., and Beckham, W.E., 1999, Detection and analysis of naturally fractured gas reservoirs: Multiazimuth seismic surveys in the Wind River basin, Wyoming: Geophysics, **64**, 1277–1292.

Horne, S., and Leaney, S., 2000, Short note: Polarization and slowness component inversion for TI anisotropy: Geophys. Prosp., **48**, 779-788.

Lynn, H.B., Beckham, W.E., Simon, K.M., Bates, C.R., Layman, M., and Jones, M., 1999, P-wave and S-wave azimuthal anisotropy at a naturally fractured gas reservoir, Bluebell-Altamont Field, Utah: Geophysics, **64**, 1312–1328.

Nichols, D., Muir, F., and Schoenberg, M., 1989, Elastic properties of rocks with multiple sets of fractures: 59th Ann. Internat. Mtg., Soc. Expl. Geophys., Expanded Abstracts, 471–474.

Pérez, M.A., Grechka, V., and Michelena, R.J., 1999, Fracture detection in a carbonate reservoir using a variety of seismic methods: Geophysics, **64**, 1266–1276.

Schoenberg, M., 1980, Elastic wave behavior across linear slip interfaces: J. Acoust. Soc. Am., **68**, 1516–1521.

Schoenberg, M., 1983, Reflection of elastic waves from periodically stratified media with interfacial slip: Geophys. Prosp., **31**, 265–292.

Schoenberg, M., and Muir, F., 1989, A calculus for finely layered anisotropic media: Geophysics, **54**, 581–589.

Schoenberg, M., and Sayers, C., 1995, Seismic anisotropy of fractured rock: Geophysics, **60**, 204–211.

Schoenberg, M., and Helbig, K., 1997, Orthorhombic media: Modeling elastic wave behavior in vertically fractured earth: Geophysics, **62**, 1954–1974.

Schoenberg, M., Dean, S., and Sayers, C.M., 1999, Azimuth-dependent tuning of seismic waves reflected from fractured reservoirs: Geophysics, **64**, 1160–1171.

Tsvankin, I., 1997, Anisotropic parameters and P-wave velocity for orthorhombic media: Geophysics, **62**, 1292–1309.

Tsvankin, I., 2001, Seismic signatures and analysis of reflection data in anisotropic media: Elsevier Science.

Tsvankin, I., and Grechka, V., 2000a, Dip moveout of converted waves and parameter estimation in transversely isotropic media: Geophysical Prospecting, **48**, 257–292.

Tsvankin, I., and Grechka, V., 2000b, Two approaches to anisotropic velocity analysis of converted waves: 70th Ann. Internat. Mtg., Soc. Expl. Geophys., Expanded Abstracts, 1193–1196.

Winterstein, D.F., 1990, Velocity anisotropy terminology for geophysicists: Geophysics, **55**, 1070–1088.

APPENDIX A: Compliance matrix of a general, arbitrarily oriented fracture set

Here, we give exact expressions for the compliance matrix $\boldsymbol{s}_f$ of a set of general (micro-corrugated) fractures with arbitrary orientation. The fracture planes are orthogonal to the unit vector $\boldsymbol{n}$ defined by the azimuth α and tilt β in the Cartesian coordinate frame $\{x_1,\, x_2,\, x_3\}$ (Figure 1):

$$\boldsymbol{n} = \{\cos\alpha\,\cos\beta,\;\; \sin\alpha\,\cos\beta,\;\; -\sin\beta\,\} \tag{A1}$$

To obtain $\boldsymbol{s}_f$, we apply an appropriate rotation to the compliance matrix $\boldsymbol{s}_f^{\mathrm{GN},\,x_1}$ [equation (5)] of a general fracture set orthogonal to the x_1-axis ($\boldsymbol{n}^{x_1} = \{1,\,0,\,0\}$). This operation includes two steps – the rotation $\boldsymbol{A}^\beta$ by the angle β around the x_2-axis and the rotation $\boldsymbol{A}^\alpha$ by the angle α around the x_3-axis – and is described by the matrix

$$\begin{aligned}\boldsymbol{A} = \boldsymbol{A}^\alpha\,\boldsymbol{A}^\beta &= \begin{pmatrix} \cos\alpha & -\sin\alpha & 0 \\ \sin\alpha & \cos\alpha & 0 \\ 0 & 0 & 1 \end{pmatrix} \begin{pmatrix} \cos\beta & 0 & \sin\beta \\ 0 & 1 & 0 \\ -\sin\beta & 0 & \cos\beta \end{pmatrix} \\ &= \begin{pmatrix} \cos\alpha\,\cos\beta & -\sin\alpha & \cos\alpha\,\sin\beta \\ \sin\alpha\,\cos\beta & \cos\alpha & \sin\alpha\,\sin\beta \\ -\sin\beta & 0 & \cos\beta \end{pmatrix}. \end{aligned} \tag{A2}$$

The corresponding transformation of the compliance matrix $\boldsymbol{s}_f^x$ (known as the Bond transformation) has the form

$$\boldsymbol{s}_f = \boldsymbol{B}\,\boldsymbol{s}_f^{\mathrm{GN},\,x_1}\,\boldsymbol{B}^T. \tag{A3}$$

An explicit expression for the 6×6 matrix $\boldsymbol{B}$ is given in Winterstein (1990), and $\boldsymbol{B}^T$ denotes the transposed matrix. Evaluating equation (A3) yields the following 6×6 symmetric matrix $\boldsymbol{s}_f$:

$$\begin{aligned} s_{11f} &= \cos^2\alpha\,\cos^2\beta\,\Big[K_H\,\sin^2\alpha - \sin 2\alpha\,(K_{NH}\,\cos\beta + K_{VH}\,\sin\beta) \\ &\quad + \cos^2\alpha\,\left(K_N\cos^2\beta + 2\,K_{NV}\,\sin 2\beta + K_V\,\sin^2\beta\right)\Big], \end{aligned} \tag{A4}$$

$$\begin{aligned} s_{12f} &= \cos\alpha\,\cos^2\beta\,\sin\alpha\,\Big[\cos 2\alpha\,(K_{NH}\,\cos\beta + K_{VH}\,\sin\beta) \\ &\quad + \cos\alpha\,\sin\alpha\,\left(K_N\cos^2\beta + 2\,K_{NV}\,\sin 2\beta + K_V\,\sin^2\beta - K_H\right)\Big], \end{aligned} \tag{A5}$$

$$\begin{aligned} s_{13f} &= \cos\alpha\,\cos\beta\,\sin\beta\,\Big\{\sin\alpha\,(K_{VH}\,\cos\beta - K_{NH}\,\sin\beta) \\ &\quad - \cos\alpha\,\left[K_{NV}\,\cos 2\beta + (K_V - K_N)\sin\beta\,cos\beta\right]\Big\}, \end{aligned} \tag{A6}$$

$$\begin{aligned} s_{14f} &= \cos\alpha\,\cos\beta\,\Big\{-\cos^2\alpha\,\sin\beta\,(K_{NH}\,\cos\beta + K_{VH}\,\sin\beta) \\ &\quad + \sin\alpha\,\cos\alpha\,\left[K_{NV}\,\cos 3\beta + \sin\beta\,(K_H - K_N + (K_V - K_N)\cos 2\beta)\right] \\ &\quad + \sin^2\alpha\,(K_{NH}\,\sin 2\beta - K_{VH}\,\cos 2\beta)\Big\}, \end{aligned} \tag{A7}$$

$$\begin{aligned} s_{15f} &= \cos\alpha\,\cos\beta\,\Big\{\cos\alpha\,\cos\beta\,\sin\alpha\,(3\,K_{NH}\,\sin\beta - K_{VH}\,\cos\beta) \\ &\quad + \cos^2\alpha\,\left[K_{NV}\,\cos 3\beta - \sin\beta\,(K_N + (K_N - K_V)\cos 2\beta)\right] \\ &\quad + \sin\beta\,\left(K_{VH}\,\sin 2\alpha\,\sin\beta - K_H\,\sin^2\alpha\right)\Big\}, \end{aligned} \tag{A8}$$

$$\begin{aligned} s_{16f} &= \cos\alpha\,\cos^2\beta\,\Big[K_H\,\sin^3\alpha + \cos\alpha\,\left(1 - 4\,\sin^2\alpha\right)(K_{NH}\,\cos\beta + K_{VH}\,\sin\beta) \\ &\quad + \cos^2\alpha\,\sin\alpha\,\left(2\,K_N\,\cos^2\beta + 2\,K_{NV}\,\sin 2\beta + 2\,K_V\,\sin^2\beta - K_H\right)\Big], \end{aligned} \tag{A9}$$

$$s_{22f} = \cos^2\beta\,\sin^2\alpha\,\Big(K_H\,\cos^2\alpha + K_N\,\cos^2\beta\,\sin^2\alpha + K_{NH}\,\cos\beta\,\sin 2\alpha$$

$$+ K_{VH}\,\sin 2\alpha\,\sin\beta + K_V\,\sin^2\alpha\,\sin^2\beta + K_{NV}\,\sin^2\alpha\,\sin 2\beta\Big)\,, \tag{A10}$$

$$\begin{aligned} s_{23f} &= \cos\beta\,\sin\alpha\,\sin\beta\Big\{\cos\alpha\,(K_{NH}\,\sin\beta - K_{VH}\,\cos\beta) \\ &- \sin\alpha\,[\,K_{NV}\,\cos 2\beta + (K_V - K_N)\,\sin\beta\,\cos\beta\,]\Big\}\,, \end{aligned} \tag{A11}$$

$$\begin{aligned} s_{24f} &= \frac{\cos\beta\,\sin\alpha}{4}\Big\{4\,K_{NV}\,\cos 3\beta\,\sin^2\alpha \\ &- 4\,\sin\beta\,\left[\,K_H\,\cos^2\alpha + K_N\,\sin^2\alpha + (K_N - K_V)\sin^2\alpha\,\cos 2\beta\,\right] \\ &+ \sin 2\alpha\,(3\,K_{VH}\,\cos 2\beta - 3\,K_{NH}\,\sin 2\beta - K_{VH})\Big\}\,, \end{aligned} \tag{A12}$$

$$\begin{aligned} s_{25f} &= \cos\beta\,\sin\alpha\Big\{\sin\alpha\,\sin\beta\,[\,K_H\,\cos\alpha + (K_{NH}\,\cos\beta + K_{VH}\,\sin\beta)\sin\alpha\,] \\ &- 2\,\cos\alpha\,\cos\beta\,\sin\beta\,[\,K_{NH}\,\cos\alpha + (K_N\,\cos\beta + K_{NV}\,\sin\beta)\sin\alpha\,] \\ &+ \cos\alpha\,\cos 2\beta\,[\,K_{VH}\,\cos\alpha + (K_{NV}\,\cos\beta + K_V\,\sin\beta)\sin\alpha\,]\Big\}\,, \end{aligned} \tag{A13}$$

$$\begin{aligned} s_{26f} &= \cos^2\beta\,\sin\alpha\Big\{\sin\alpha\,\left(4\,\cos^2\alpha - 1\right)(K_{NH}\,\cos\beta + K_{VH}\,\sin\beta) \\ &- \cos\alpha\,\sin^2\alpha\,[\,K_H - K_N - K_V + (K_V - K_N)\,\cos 2\beta - 2\,K_{NV}\,\sin 2\beta\,] \\ &+ K_H\,\cos^3\alpha\Big\}\,, \end{aligned} \tag{A14}$$

$$s_{33f} = \sin^2\beta\,\left(K_V\,\cos^2\beta - K_{NV}\,\sin 2\beta + K_N\,\sin^2\beta\right)\,, \tag{A15}$$

$$\begin{aligned} s_{34f} &= -\sin\beta\Big\{K_V\,\cos^3\beta\,\sin\alpha - 3\,K_{NV}\,\cos^2\beta\,\sin\alpha\,\sin\beta \\ &+ \sin^2\beta\,(K_{NH}\,\cos\alpha + K_{NV}\,\sin\alpha\,\sin\beta) \\ &- \cos\beta\,\sin\beta\,[\,K_{VH}\,\cos\alpha + (K_V - 2\,K_N)\sin\alpha\,\sin\beta\,]\Big\}\,, \end{aligned} \tag{A16}$$

$$\begin{aligned} s_{35f} &= -\sin\beta\Big\{\sin\alpha\,\sin\beta\,(K_{VH}\,\cos\beta - K_{NH}\,\sin\beta) \\ &+ \frac{\cos\alpha}{2}\,[\,(K_V + K_N)\cos\beta + (K_V - K_N)\,\cos 3\beta - 2\,K_{NV}\,\sin 3\beta\,]\Big\}\,, \end{aligned} \tag{A17}$$

$$\begin{aligned} s_{36f} &= \sin\beta\,\cos\beta\Big\{\cos 2\alpha\,(K_{NH}\,\sin\beta - K_{VH}\,\cos\beta) \\ &- \sin 2\alpha\,[\,K_{NV}\,\cos 2\beta + (K_V - K_N)\,\sin\beta\,\cos\beta\,]\Big\}\,, \end{aligned} \tag{A18}$$

$$\begin{aligned} s_{44f} &= K_V\,\cos^4\beta\,\sin^2\alpha - 4\,K_{NV}\,\cos^3\beta\,\sin^2\alpha\,\sin\beta \\ &+ 4\,\cos\beta\,\sin\alpha\,\sin^2\beta\,(K_{NH}\,\cos\alpha - K_{NV}\,\sin\alpha\,\sin\beta) \\ &- 2\,\cos^2\beta\,\sin\alpha\,\sin\beta\,[\,K_{VH}\,\cos\alpha + (K_V - 2\,K_N)\,\sin\alpha\,\sin\beta\,] \\ &+ \sin^2\beta\,\left[\,K_H\,\cos^2\alpha + (K_{VH}\,\sin 2\alpha + K_V\,\sin^2\alpha\,\sin\beta)\,\sin\beta\,\right]\,, \end{aligned} \tag{A19}$$

$$\begin{aligned} s_{45f} &= -\cos 2\alpha\,\sin\beta\,(K_{VH}\,\cos 2\beta - K_{NH}\,\sin 2\beta) \\ &- \frac{\sin 2\alpha}{4}\,\Big[\,K_V + K_N + (K_V - K_N)\,\cos 4\beta \\ &- 2\,K_H\,\sin^2\beta - 2\,K_{NV}\,\sin 4\beta\,\Big]\,, \end{aligned} \tag{A20}$$

$$
\begin{aligned}
s_{46f} = \cos\beta \Big\{ & \cos 2\alpha \Big[K_{VH} \cos^2\beta \sin\alpha - 2 K_{NH} \cos\beta \sin\alpha \sin\beta \\
& - \sin\beta \left(K_H \cos\alpha + K_{VH} \sin\alpha \sin\beta\right) \Big] \\
& - 2 \cos\alpha \sin\alpha \Big[\left(2 K_N - K_V\right) \cos^2\beta \sin\alpha \sin\beta - K_{NV} \cos^3\beta \sin\alpha \\
& + \cos\beta \sin\beta \left(K_{NH} \cos\alpha + 3 K_{NV} \sin\alpha \sin\beta\right) \\
& + \sin^2\beta \left(K_{VH} \cos\alpha + K_V \sin\alpha \sin\beta\right) \Big] \Big\},
\end{aligned} \tag{A21}
$$

$$
\begin{aligned}
s_{55f} = & -\sin 2\alpha \sin^2\beta \left(2 K_{NH} \cos\beta + K_{VH} \sin\beta\right) \\
& + \sin\beta \left(K_{VH} \cos^2\beta \sin 2\alpha + K_H \sin^2\alpha \sin\beta\right) \\
& + \frac{\cos^2\alpha}{2} \left[K_V + K_N + \left(K_V - K_N\right) \cos 4\beta - 2 K_{NV} \sin 4\beta \right],
\end{aligned} \tag{A22}
$$

$$
\begin{aligned}
s_{56f} = \cos\beta \Big\{ & K_H \cos 2\alpha \sin\alpha \sin\beta \\
& + \cos^2\alpha \sin\alpha \left[2 K_{NV} \cos 3\beta - 2 \left(K_N + \left(K_N - K_V\right) \cos 2\beta\right) \sin\beta \right] \\
& + \cos\alpha \Big[2 \sin^2\alpha \sin\beta \left(K_{NH} \cos\beta + K_{VH} \sin\beta\right) \\
& + \cos 2\alpha \left(K_{VH} \cos 2\beta - K_{NH} \sin 2\beta\right) \Big] \Big\},
\end{aligned} \tag{A23}
$$

$$
\begin{aligned}
s_{66f} = \cos^2\beta \Big\{ & K_H \left(\cos^4\alpha + \sin^4\alpha\right) + 2 \sin 2\alpha \left(K_{NH} \cos\beta + K_{VH} \sin\beta\right) \\
& - \frac{\sin^2 2\alpha}{2} \left[K_H - K_N - K_V + \left(K_V - K_N\right) \cos 2\beta - 2 K_{NV} \sin 2\beta \right] \Big\}.
\end{aligned} \tag{A24}
$$

Equations (A4)–(A24) are derived for the most general fracture rheology described by six independent excess fracture compliances. The matrices $\boldsymbol{s}_f$ for diagonal [equation (7)] or rotationally invariant [equation (9)] fractures can be obtained by substituting the corresponding constraints (8) and (10).